

# RETRACTED ARTICLE: LINC00261 Inhibits Esophageal Cancer Radioresistance by Down-Regulating microRNA-552-3p and Promoting DIRAS1

Baolong Yang  
Hongbing Ma   
Yan Bian

Department of Radiotherapy Oncology,  
The Second Affiliated Hospital of Xi 'an  
Jiaotong University, Xi 'an, Shanxi  
Province, 710004, People's Republic of  
China

**Objective:** Esophageal cancer (EC) represents a life-threatening tumor with an ever-increasing incidence rate. Long intergenic non-protein coding RNAs (LINC) have also become a topic of interest in EC. In a similar light, the current study aimed to investigate the role of LINC00261 in EC radioresistance.

**Methods:** Firstly, radioresistant EC cell lines TE-1-R and TE-5-R were established using TE-1 and TE-5 cells. Subsequently, LINC00261, microRNA (miR)-552-3p, and DIRAS1 expression patterns in EC tissues and adjacent normal tissues and EC cells were evaluated. In addition, survival fraction (SF), colony formation, apoptosis, and  $\gamma$ -H2AX levels were analyzed, followed by the detection of the binding relation between LINC00261 and miR-552-3p and between miR-552-3p and DIRAS1. Lastly, xenograft transplantation was carried out to confirm the effects of LINC00261 on EC radioresistance in vivo.

**Results:** LINC00261 and DIRAS1 were poorly-expressed in EC tissues and cells, but miR-552-3p was over-expressed. In EC cells with X-ray radiation, over-expression of LINC00261 reduced SF and cell viability, strengthened  $\gamma$ -H2AX levels, and promoted apoptosis, while all these trends were counteracted by miR-552-3p over-expression or DIRAS1 silencing. Mechanistic investigation further validated the binding relation between LINC00261 and miR-552-3p, and between miR-552-3p and DIRAS1. Moreover, LINC00261 over-expression suppressed tumor growth and reduced EC radioresistance in vivo.

**Conclusion:** Altogether, our findings indicated that LINC00261 exerts a suppressive effect on EC radioresistance via the competing endogenous RNA network to sponge miR-552-3p and up-regulate DIRAS1 transcription.

**Keywords:** esophageal cancer, radioresistance, long intergenic non-protein coding RNA 00261, microRNA-552-3p, DIRAS1, TE-1-R

## Introduction

Esophageal cancer (EC), regarded as one of the most prevalent and malignant tumors across the world, is associated with extremely high incidence and mortality rates, in addition to geographic variability, high aggressiveness, and exasperating prognostic outcomes.<sup>1</sup> Nowadays, EC is well known as multifactorial cancer that can be precipitated by various factors, such as micronutrient deficiency, gastroesophageal diseases, smoking, alcohol consumption, obesity, spicy foods, excessive nitrosamines, and even poor socioeconomic status.<sup>2</sup> Clinically, treatment options for EC comprise endoscopic resection, minimally invasive esophagectomy, salvage esophageal resection, chemotherapy, and radiotherapy.<sup>3</sup> Although chemotherapy

Correspondence: Hongbing Ma; Yan Bian  
Department of Radiotherapy Oncology,  
The Second Affiliated Hospital of Xi 'an  
Jiaotong University, Xiwu Road No. 157,  
Xi 'an, Shanxi Province, 710004, People's  
Republic of China  
Tel +86-13991845066  
Email mahongbing0530@163.com;  
mcgddaxnaand0lxkx@163.com

and radiotherapy can bring about delayed tumor growth and enhanced prognostic results, the advent of chemoresistance or radioresistance imposes damage to patients with EC and hinders the overall curative effect.<sup>4</sup> Therefore, it would be prudent to explore the underlying mechanism of EC radioresistance to improve the quality of life of EC patients.

As an integral member of the long non-coding RNA (lncRNA) family, long intergenic non-protein coding RNAs (LINC)s are well-established to be implicated in cancer oncogenesis, progression, treatment, and clinical consequences.<sup>5</sup> What's more, LINC dysregulation can also confer effects on EC initiation, development, metastasis, aggressiveness, cell renewal, and chemoradiotherapy resistance, due to its ability to recruit complexes to chromatin, modulate gene expressions, and regulate the interplay between RNAs and proteins.<sup>6</sup> One such LINC, namely LINC00261, is known to be insufficiently expressed in a wide variety of cancers, ranging from pancreatic cancer, colon cancer, to prostate cancer, while newer studies have also implicated LINC00261 with cancer cell viability, mobility radioresistance, and poor prognosis.<sup>7–9</sup> Regarding EC, LINC00261 can promote EC cell sensitivity to drugs, whereas, silencing of LINC00261 was previously shown to augment EC growth and diminish apoptosis and sensitivity.<sup>10</sup> Mechanistic-based studies have also indicated that LINC00261 can mediate tumorigenesis and cancer progression by means of competing endogenous RNA (ceRNA) interactions.<sup>11,12</sup> Inherently, the ceRNA interaction is comprised of lncRNAs, microRNAs (miRNAs), circular RNAs, mRNAs, and proteins, and renders critical effects on neoplasm development.<sup>13</sup> Then, we explore the downstream miRs involved in EC. Furthermore, up-regulation of miR-552 is a common occurrence in a large number of malignancies, when an abundant miR-552 can affect cancer cell survival, transcription, mobility, dissemination, propagation, invasiveness, death and resistance, and sensitivity to drugs.<sup>14</sup> Recent studies have further highlighted miR-552-3p as a valuable diagnostic and prognostic biomarker in digestive tract malignancies, including EC.<sup>15</sup> Lastly, DIRAS family GTPase 1 (DIRAS1), represents a member of the RAS superfamily and serves as an inhibitor of human cancers.<sup>16</sup> It is also noteworthy that DIRAS1 has been previously suggested as a putative inhibitor in EC.<sup>17</sup> Consequently, the current study set out to explore the specific role of LINC00261 in EC radiosensitivity via interaction with the miR-552-3p/DIRAS1 axis.

## Materials and Methods

### Ethics Statement

The current study was approved and supervised by the Ethics committee of The Second Affiliated Hospital of Xi'an Jiaotong University. Signed informed consents were obtained from all participants prior to specimen collection. Animal experimentation protocols were approved by the Institutional Animal Care and Use Committee of The Second Affiliated Hospital of Xi'an Jiaotong University, and conformed to the Guidelines for the Care and Use of Laboratory Animals. Each step was conducted in accordance with the Declaration of Helsinki. Significant efforts were made to minimize both the number of animals and their respective suffering.

### Tissue Collection

Firstly, endoscopic biopsy specimens (69 EC tissue specimens and 69 paracancerous tissues) were obtained from 69 EC patients (comprising of 43 males and 26 females) diagnosed at The Second Affiliated Hospital of Xi'an Jiaotong University from June 2016 to June 2018. The inclusion criteria were as follows: I) no patients received anticancer treatment prior to tissue collection; II) no patients were complicated with other malignancies or chronic infectious diseases; III) there were no tissue lesions in paracancerous tissues; and IV) patients presented with complete clinical information such as age, gender, medical history, and treatment plan. Exclusion criteria were as follows: I) non-completed 3-year follow-up; II) accidental death due to other diseases; III) pregnancy, breastfeeding, or drug addiction; and IV) patients undergoing other types of medical treatment, such as participation in and withdrawal from the clinical experiment of other drugs or biological therapies. All EC patients underwent radiotherapy after surgery. Depending on the condition of patients, doses of 50–66 Gy were prescribed, followed by administration of fractional doses of 2 Gy/d once a day, 5 times a week for 6–7 weeks. Patients were treated using a Varian 23EX and a 120-leaf MLC 600C/D linear accelerator. Subsequently, the collected EC specimens were divided into the radiation sensitive group (N=47) and the radiation resistant group (N=22), in accordance with the response evaluation criteria.<sup>19</sup>

### Cell Culture

Human normal esophageal cell line (HEEC) and human EC cell lines (TE-1, TE-5, ECA109, and KYSE150) were

**Table 1** Primer Sequence of RT-qPCR

	Forward Primer (5'-3')	Reverse Primer (5'-3')
LINC00261	CGTAGTGATAGTCCCGTGCC	TGGCAAGACGGATGGAACA
miR-552-3p	GCCGAGGCGGAGCGCCTG	CTCAACTGGTGTCTGTGGA
DIRAS1	CAGGGTATCTGGGGAATGGC	GTCCATAATGAGAGGCAGGGA
U6	CGCACTTTACGGCTACCTCT	GCGACAAGGGAAGGGAACAA
GAPDH	GCATCTTCTTGTGCAGTGCC	TACGGCCAATCCGTTCA

**Abbreviations:** RT-qPCR, reverse transcription-quantitative polymerase chain reaction; LINC00261, long intergenic non-protein coding RNA; miR, microRNA; DIRAS1, DIRAS family GTPase 1; GAPDH, glyceraldehyde-3-phosphate dehydrogenase.

all procured obtained from Shanghai Yaji Biotechnology Co., Ltd. (Shanghai, China). Subsequently, the adherent cells were cultured in Roswell Park Memorial Institute-1640 medium (Wuhan Procell Life Technology Co., Ltd, Wuhan, Hubei, China) containing 10% fetal bovine serum, 100 U/mL penicillin, and 100 µg/mL streptomycin in a 37°C incubator with 5% CO<sub>2</sub> in air and saturated humidity. The medium was refreshed every other day, and cells at the logarithmic phase of growth were selected for subsequent experiments.

Afterwards, TE-1 and TE-5 cells were cultured in 6-well plates for 24 h, and then infected with lentivirus (LV)-packaged over-expression of LINC00261 vector pcDNA3.1-LINC00261 (oe-LINC00261) or the empty vector pcDNA3.1-negative control (oe-NC) (GenePharma, Shanghai, China) at a multiplicity of infection of 50 per cell. Next, the cells were then transfected with miR-552-3p mimic or mimic-NC, small interfering (si) DIRAS1 or si-NC (GenePharma) using 200 ng Lipofectamine 2000 (Invitrogen Inc., Carlsbad, CA, USA) according to the manufacturer's instructions.

## Establishment of Radioresistance Cell Lines

TE-1 and TE-5 cells at the logarithmic phase of growth were passaged in a 25 cm<sup>2</sup> cell culture flask. Upon reaching 50% confluence, the adherent cells were irradiated with 2 Gy X-rays and cultured in a 37°C incubator with 5% CO<sub>2</sub> in air. Upon reaching 90% (2–3 d), the cells were isolated for passaging. When cell confluence reached 50% again, the cells were irradiated with 2 Gy X-ray and incubated in a 37°C incubator with 5% CO<sub>2</sub> in air. The cells were irradiated several times, as described above, at a total dose of 50 Gy (25 × 2 Gy), and the irradiated cells were regarded as TE-1-R and TE-5-R. Throughout the process, the parent cells, namely TE-1, were passaged in the same manner, with the exception of X-ray irradiation.

## Reverse Transcription-Quantitative Polymerase Chain Reaction (RT-qPCR)

Total RNA content was extracted from cells using the TRIzol reagent in accordance with the manufacturer's instructions. Subsequently, RNA concentration was determined with a NanoDrop spectrophotometer (Thermo Fisher Scientific, Rockford, IL, USA). Afterwards, the complementary DNA was reverse-transcribed using RT kit (Promega Inc., Burlington, ON, Canada). RT-qPCR was then carried out using Power SYBRgreen PCR master Mix (Life Technologies; Thermo Fisher Scientific, Waltham, MA, USA). The primers synthesized by Shanghai Sangon (Shanghai, China) are listed in Table 1. The relative expression was calculated using the 2<sup>-ΔΔCt</sup> method.

## Cell Counting Kit-8 (CCK-8) Assay

Cell proliferation in different groups was evaluated using CCK-8 kits (Dojindo Molecular Technologies, Rockville, MD, USA), in accordance with the manufacturer's instructions. Briefly, cells (3 × 10<sup>3</sup> cells/well) were seeded in 96-well plates overnight until cells were adherent. Next, the cells were irradiated with 0, 2, 4, 6, and 8 Gy X-ray, respectively, and cell viability was assessed 72 h after irradiation. Subsequently, the cells were cultured with CCK-8 solution (10 µg/mL, Dojindo) in a 37°C humidified incubator with 5% CO<sub>2</sub> in air. Afterwards, the optical density at the wavelength of 450 nm was detected with the help of a microplate reader (Bio-Rad, Hercules, CA, USA).

## Colony Formation Assay

Cell suspension (2 × 10<sup>3</sup>) was seeded in 6-well plates, followed by X-ray irradiation at 4 Gy. Following irradiation, the cells were cultured for 14 days till the appearance of colonies. Next, the colonies were subjected to a 15 min-fixation with 4% methyl alcohol and 30 min-staining with

1% Giemsa (AppliChem, Darmstadt, Germany), followed by counting of the number of colonies containing more than 50 cells. Each procedure was independently performed 3 times to obtain the mean value.

## Flow Cytometry

Cells ( $3 \times 10^5$  cells/well) were seeded in 6-well plates. Upon reaching 60% cell density, the cells were irradiated with 4 Gy X-ray, followed by 24 h of culture. Next, the cells were collected in 1.5 mL EP tubes and centrifuged at  $2000 \times g$  at  $4^\circ\text{C}$  to discard the supernatant. Afterwards, the cells were suspended with 500  $\mu\text{L}$  binding buffer and cultured with 5  $\mu\text{L}$  Annexin V-fluorescein isothiocyanate (FITC) at  $4^\circ\text{C}$  for 30 min. Later, the cells were incubated with 5  $\mu\text{L}$  propidium iodide for 5 min at room temperature. Following incubation, apoptosis was detected with the help of Annexin-V-FITC assay kits (K201-100, BioVision Inc., Mountain View, CA, USA) and flow cytometry (version 10.0, FlowJo, FACS Calibur<sup>TM</sup>, BD, USA).

## Immunofluorescent Staining

Immunofluorescent staining was performed in compliance with the standard protocols. Briefly, the cells were fixed with 4% paraformaldehyde, permeated using 0.2% Triton X-100, and blocked with 5% bovine serum albumin at room temperature for 1 h. Next, the cells were incubated with rabbit anti-human  $\gamma$ -H2AX antibody (dilution ratio of 1:250, ab81299, Abcam Inc., Cambridge, MA, USA) overnight at  $4^\circ\text{C}$ , cultured with fluorescent staining coupled secondary antibody (dilution ratio of 1:1000, ab759, Abcam) for 1 h, followed by staining with 4',6-diamidino-2-phenylindole. Finally, the cells were photographed and observed under a Zeiss microscope (Zeiss Inc, AG, Oberkochen, Germany).

## Bioinformatics

Subcellular localization of LINC00261 was predicted using the iLocate website (<http://www.csbio.sjtu.edu.cn/bioinf/locate/>/?tdsourcetag=s\_pcqq\_aiomsg).

Additionally, the target genes downstream LINC00261 and miR-552-3p and their corresponding binding sites were predicted using the LncBasev.2 ([http://carolina.imis.athena-innovation.gr/diana\\_tools/web/index.php?r=lncbasev2%2Findex-predicted](http://carolina.imis.athena-innovation.gr/diana_tools/web/index.php?r=lncbasev2%2Findex-predicted)), StarBase (<http://starbase.sysu.edu.cn/index.ph>), LNCRNASNP2 (<http://bioinfo.life.hust.edu.cn/lncRNASNP#!/>), RNA22 (<https://cm.jefferson.edu/rna22/Precomputed/>), miRTarBase (<http://miRTarBase.cuhk.edu.cn/>), and miRWalk (<http://mirwalk.umm.uni-heidelberg.de/>) databases.

## Fractionation of Nuclear and Cytoplasmic RNA

Cytoplasmic and Nuclear RNA purification kits (Norgenbiotek Corporation, Thorold, ON, Canada) were adopted for the subcellular fractionation of RNA from TE-1 cells, in accordance with the manufacturer's instructions. Afterwards, cytoplasmic and nuclear fractions were detected by means of RT-qPCR.

## Dual-Luciferase Reporter Gene Assay

Wild type (WT) and mutant type (MUT) LINC00261 and DIRAS1 fragments containing the binding sites of miR-552-3p were constructed and cloned into the psiCHECK-2 vector (Hambio Biotechnology Co., Ltd, Shanghai, China). Next, the constructed dual-luciferase reporter plasmids were cotransfected with mimic-NC or miR-552-3p-mimic into 293T cells. After 48 h, the cells were collected and evaluated using a dual-luciferase reporter gene assay system (Promega, Madison, WI, USA).

## RNA Pull-Down Assay

TE-1 cells were digested with trypsin and lysed in RNA-binding protein immunoprecipitation (RIP) lysis buffer. Next, the lysis buffer was divided into several aliquots and frozen at  $-80^\circ\text{C}$ . Subsequently, 1  $\mu\text{g}$  biotin-labeled RNA and 500  $\mu\text{L}$  structure buffer were added into EP tubes using the RNA-protein magnetic bead sedimentation kit (Pierce, Rockford, IL). The cells were then immersed in water at  $95^\circ\text{C}$  for 2 min, soaked in ice for 3 min, cultured with 50  $\mu\text{L}$  fully resuspended beads at  $4^\circ\text{C}$  overnight with the supernatant discarded, centrifuged at 12 g for 3 min, rinsed 3 times with 500  $\mu\text{L}$  RIP cleaning solution and mixed with 10  $\mu\text{L}$  cell lysate for 1 h. Afterwards, protein in the incubated bead-RNA-protein mixture was eluted, and the protein concentration was determined using the bicinchoninic acid method. RNA expression patterns were determined by RT-qPCR.

## Xenografts Tumors in Nude Mice

A total of 36 male BALB/c nude mice (aged 4–6 weeks old, procured from Charles River, Beijing, China) were raised in 12-h light/dark cycles at  $25^\circ\text{C}$  and 60% humidity, with ad libitum access to standard food and sterile water. Subsequently, TE-1-R cells (0.2 mL,  $1 \times 10^7$  cells) infected with LV-LINC00261 or LV-NC were subcutaneously injected into the back of nude mice. After 7 d, the tumor of mice was exposed to 4 Gy of X-ray radiation. Tumor volume was



calculated every 7 days using the following formula: tumor volume = (length × width<sup>2</sup>)/2. Pentobarbital sodium (150 mg/kg) was intraperitoneally injected into mice about 35 d after the injection to euthanize the mice. Tumors were immediately removed and weighed. Tumor tissues from 6 mice in each group were adopted for RT-qPCR and the remaining 6 mice were used for immunohistochemistry (IHC).

## IHC

The levels of  $\gamma$ -H2AX and Ki67 in tumors were evaluated with the help of IHC. Briefly, tissue sections (4  $\mu$ m) were subjected to dehydration, rehydration, antigen recovery, endogenous peroxidase exhaustion, and non-specific signal blockage. Subsequently, the tissue sections were detected with anti- $\gamma$ -H2AX (dilution ratio of 1:1000, ab124781, Abcam) and anti-ki67 (dilution ratio of 1:200, ab16667, Abcam) at 4°C, and then cultured with enzyme-labeled secondary (dilution ratio of 1:500, ab150113, Abcam) at room temperature for 1 h. Afterwards, tissue sections were observed using the 2,4-diaminobutyric acid substrate, stained with hematoxylin, and then finally imaged.

## Statistical Analysis

Data analyses were performed using the GraphPad Prism 8.0 software (GraphPad Software Inc., San Diego, CA, USA). Measurement data were presented as mean  $\pm$  standard deviation. The *t*-test was applied for comparison analyses between two groups, and one-way or two-way analysis of variance (ANOVA) was adopted for comparison analysis among multiple groups, while Tukey's multiple comparisons test was

used for post-test of data. The *p* value was attained using a two-tailed test, and a value of *p* < 0.05 was regarded statistically significant.

## Results

### LINC00261 is Expressed in EC

Firstly, the TCGA database was retrieved to explore the role of LINC00261 in EC radioresistance, which revealed that LINC00261 was down-regulated in EC (Figure 1A). Subsequent detection of the EC and paracancerous tissues illustrated that LINC00261 was poorly expressed in EC tissues (*p* < 0.05; Figure 1B). EC patients undergoing treatment were further divided into the radiation sensitive group and the radiation resistant group according to the evaluation standard. We observed that the radiation resistant group presented with lower LINC00261 expression levels compared with those of the radiation sensitive group (*p* < 0.05; Figure 1C). In addition, LINC00261 expression patterns in 4 different EC cell lines were detected, which demonstrated that LINC00261 was under-expressed in all EC cell lines (*p* < 0.05; Figure 1D). Together, these findings indicated that LINC00261 was poorly-expressed in EC. Meanwhile, TE-1 cells, which exhibited the lowest LINC00261 expression, and TE-5, which exhibited the highest LINC00261 expression, were both selected for further experimentation.

### LINC00261 Over-Expression Boosts EC Cell Radiosensitivity

To further investigate the role of LINC00261 in EC radioresistance, we evaluated LINC00261 expression

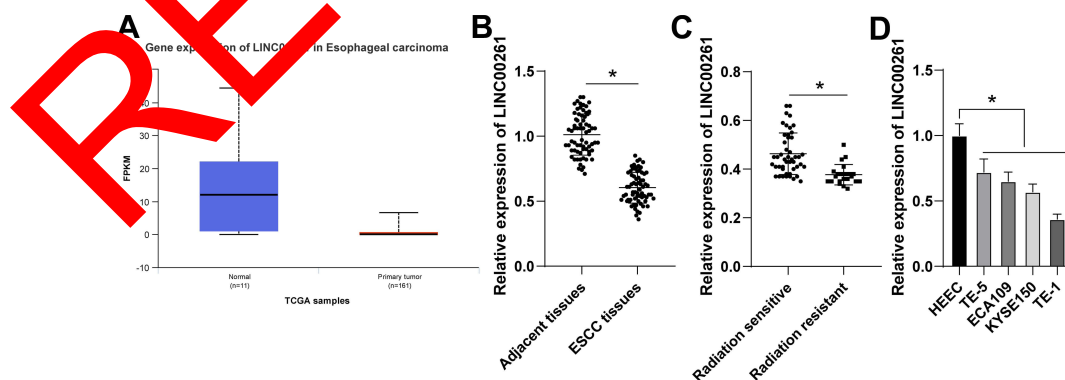


**Figure 1** LINC00261 is poorly expressed in EC. EC and paracancerous tissues were harvested from EC patients. (A) LINC00261 expression was analyzed by TCGA data. (B) LINC00261 expression in EC tissues was tested by RT-qPCR (N = 69). (C) LINC00261 expression in the radiation sensitive group (N = 47) and the radiation resistant group (N = 22) was assessed. (D) LINC00261 expression in normal and EC cells was measured by RT-qPCR. The independent cell experiment was repeated 3 times. The measurement data were presented as mean  $\pm$  standard deviation. The independent *t*-test was appointed to analyze data in (B and C). One-way ANOVA was appointed to analyze data in (D). Tukey's multiple comparisons test was employed for the post hoc test. \**p* < 0.05.

patterns in radioresistant and parental EC cell lines. It was found that compared with TE-1 and TE-5 cells, TE-1-R and TE-5-R cells presented with reduced LINC00261 expression levels ( $p < 0.05$ ; Figure 2A). Next, oe-LINC00261 was adopted to infect TE-

1-R and TE-5-R cells to up-regulate the LINC00261 expression in TE-1-R and TE-5-R cells ( $p < 0.05$ ; Figure 2B). Subsequent findings revealed that compared with the parental cells, the radioresistant cells presented with a higher survival fraction (SF) under different

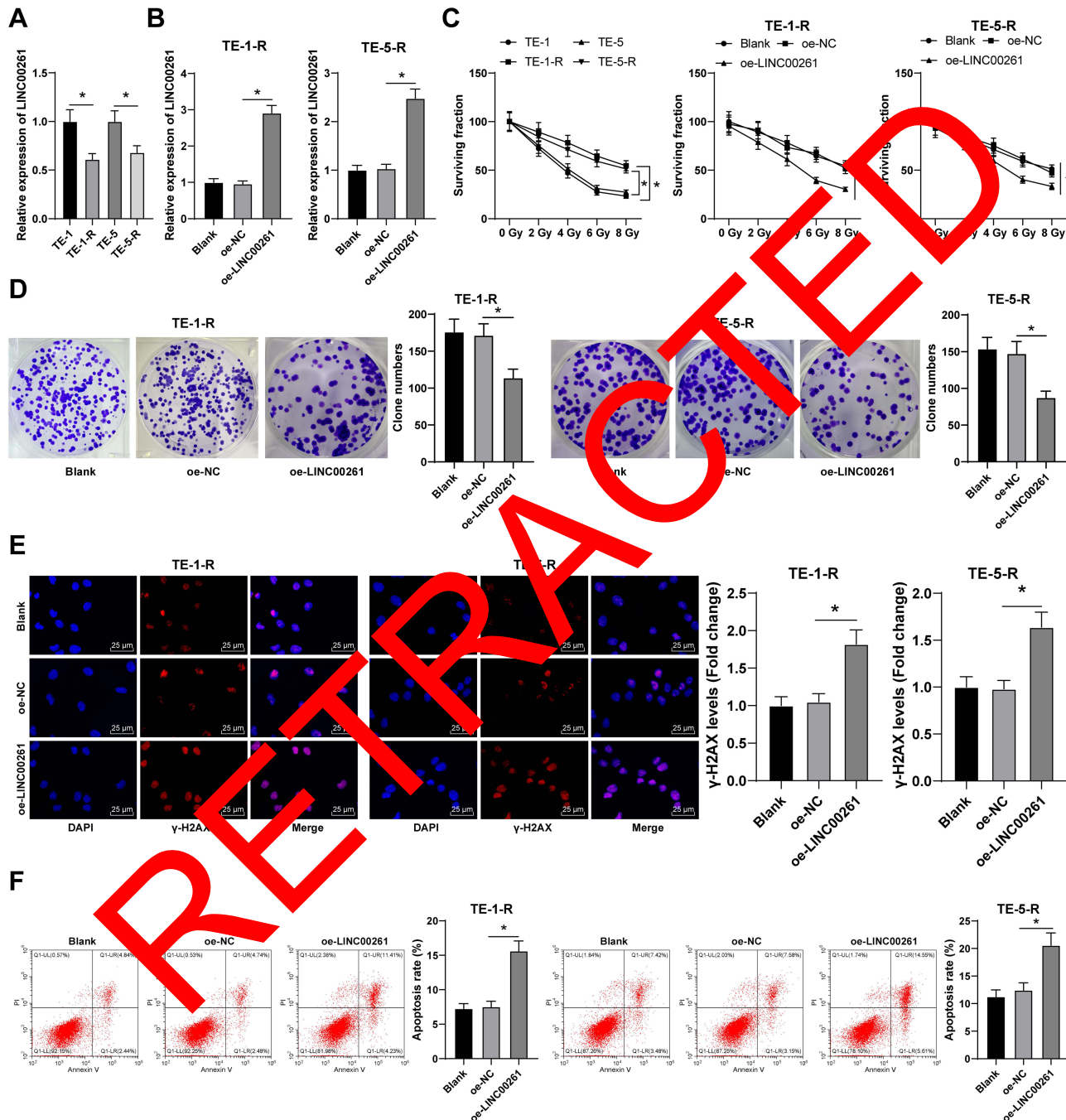


**Figure 2** LINC00261 overexpression boosts EC cell radiosensitivity. Radioresistant cell lines TE-1-R and TE-5-R were established, and cells were infected by oe-LINC00261, with cells infected with oe-NC as control. (A and B) LINC00261 expression in cells was assessed by RT-qPCR. (C) SF in each group under 0, 2, 4, 6, and 8 Gy X-ray radiation was measured by the CCK-8 method. (D) Colony formation of cells under 4 Gy X-ray radiation was determined by colony formation assay. (E)  $\gamma$ -H2AX levels of cells under 4 Gy X-ray radiation were determined by immunofluorescent staining. (F) Apoptosis of cells under 4 Gy X-ray radiation was determined by flow cytometry. The independent experiment was repeated 3 times. The measurement data were presented as mean  $\pm$  standard deviation. One-way ANOVA was appointed to analyze data in (A, B, D, E, and F). Two-way ANOVA was appointed to analyze data in (C). Tukey's multiple comparisons test was employed for the post hoc test. \* $p < 0.05$ .

radiation doses of X-ray, whereas cells with oe-LINC00261 treatment exhibited lower SF ( $p < 0.05$ ; Figure 2C). Radiation of 4 Gy X-ray, under which SF of parental cells was about 50%, was selected for further experiments. Moreover, we observed that in TE-1-R and TE-5-R cells under 4 Gy X-ray radiation and treated with oe-LINC00261, colony formation was decreased ( $p < 0.05$ ; Figure 2D),  $\gamma$ -H2AX levels were elevated ( $p < 0.05$ ; Figure 2E), and apoptosis was expedited ( $p < 0.05$ ; Figure 2F), all of which suggested that LINC00261 over-expression could improve EC cell radiosensitivity.

### LINC00261 Targets miR-552-3p

To clarify the downstream mechanism of LINC00261, the lncLocator website was adopted to predict the subcellular localization of LINC00261, which unveiled that LINC00261 was localized in the cytoplasm (Figure 3A). Afterwards, fractionation of nuclear and cytoplasmic RNA analysis verified that LINC00261 was indeed expressed at the cytoplasm (Figure 3B), suggesting that LINC00261 might modulate EC cell activities via the ceRNA network. Thereafter, the LncBase v.2, Starbase, and LNCRNASNP2 online databases were adopted to explore the downstream target of LINC00261 (Figure 3C), and miR-552-3p was found at the intersection. Existing evidence suggests that miR-552-3p is over-expressed in EC and can function as a diagnostic marker.<sup>15</sup> We further predicted the presence of a binding site between LINC00261 and miR-552-3p using the StarBase database, and the binding relation between them was validated with a dual-luciferase reporter gene assay and RNA pulldown assay ( $p < 0.05$ ; Figure 3D and E). Moreover, miR-552-3p expression patterns in EC tissues were detected, and it was found that miR-552-3p was highly-expressed in EC tissues ( $p < 0.05$ ; Figure 3F), and that miR-552-3p was negatively-related to LINC00261 ( $r = -0.751$ ,  $p = 0.001$ ; Figure 3G). In addition, detection of miR-552-3p expression patterns in 4 kinds of EC cell lines illustrated that miR-552-3p exhibited up-regulated expression levels in all EC cell lines compared to that in HECC cells ( $p < 0.05$ ; Figure 3H). Furthermore, miR-552-3p expression was found to be up-regulated in TE-1-R and TE-5-R cells as compared with those in parental cells ( $p < 0.05$ ; Figure 3I). Besides, when LINC00261 was over-expressed, miR-552-3p expression was down-regulated ( $p < 0.05$ ; Figure 3J). Altogether, these findings indicated that LINC00261 negatively-targeted miR-552-3p in EC.

### miR-552-3p Over-Expression Neutralizes the Promotive Effect of LINC00261 on EC Cell Radiosensitivity

Furthermore, we transfected the miR-552-3p-mimic or mimic-NC into TE-1-R cells ( $p < 0.05$ ; Figure 4A) to perform a collaborative experiment with oe-LINC00261. It was observed that, under 4 Gy X-ray radiation, the miR-552-3p-mimic group exhibited decreased  $\gamma$ -H2AX levels ( $p < 0.05$ ; Figure 4B), elevated colony formation ( $p < 0.05$ ; Figure 4C), and reduced apoptosis ( $p < 0.05$ ; Figure 4D) compared to the oe-LINC00261 group. Overall, these findings indicated that miR-552-3p over-expression neutralized the promotive effect of LINC00261 on EC cell radiosensitivity.

### miR-552-3p Targets DIRAS1

Additionally, we explored the downstream regulation mechanism of miR-552-3p with the help of the StarBase, RNA22, miRTarBase, and miWalk online databases (Figure 5A), and DIRAS1 was found at the intersection. Existing evidence suggests that DIRAS1 serves as an inhibitor of esophageal squamous cancer.<sup>20</sup> The binding site between miR-552-3p and DIRAS1 was predicted with the StarBase website, and the binding relation between them was verified by a dual-luciferase reporter gene assay ( $p < 0.05$ ; Figure 5B). Besides, DIRAS1 expression levels were found to be lower in EC tissues relative to paracancerous tissues ( $p < 0.05$ ; Figure 5C), while DIRAS1 was positively-correlated with LINC00261 ( $r = 0.611$ ,  $p < 0.001$ ) and negatively-correlated with miR-552-3p ( $r = -0.747$ ,  $p < 0.001$ , Figure 5D). Moreover, it was observed that DIRAS1 mRNA was poorly-expressed in EC cells as compared to that in HECC cells ( $p < 0.05$ ; Figure 5E), while also being down-regulated in TE-1-R and TE-5-R cells as compared to those in parental cells ( $p < 0.05$ ; Figure 5F). Together, these findings indicated LINC00261 over-expression led to an elevated DIRAS1 expression; while miR-552-3p over-expression brought about the opposing trends in DIRAS1 levels ( $p < 0.05$ ; Figure 5G).

### DIRAS1 Depletion Partially Annuls the Promotive Role of LINC00261 Over-Expression in EC Cell Radiosensitivity

We further transfected TE-1-R cells with si-DIRAS1 or si-NC ( $p < 0.05$ ; Figure 6A) to perform collaborative

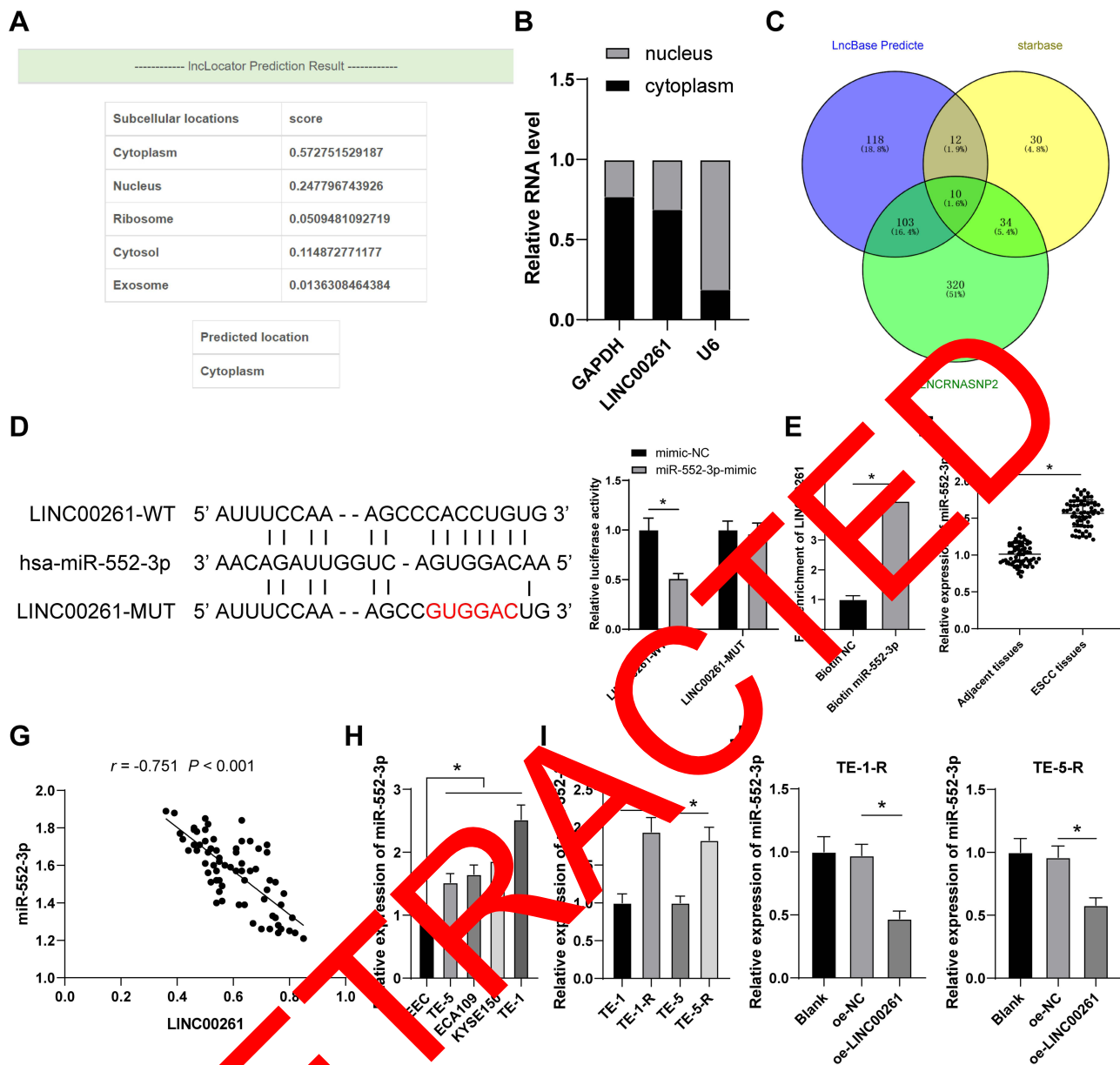


**Figure 3** LINC00261 targets miR-552-3p. (A) Subcellular localization of LINC00261 was predicted by an online tool LncLocator. (B) LINC00261 location in TE-1 cells was analyzed by fractionation of nuclear and cytoplasmic RNA analysis. (C) Target genes downstream of LINC00261 were analyzed by LncBase v.2, Starbase, and LNCRNASNP2 websites. (D and E) The binding relationship between LINC00261 and miR-552-3p was verified by dual-luciferase reporter gene assay (D) and pull-down assay (E). (F) miR-552-3p expression in EC tissues was measured by RT-qPCR. (G) The correlation analysis of LINC00261 and miR-552-3p. (H and I) miR-552-3p expression in EC cells was determined by RT-qPCR. The independent experiment was repeated 3 times. The measurement data were presented as mean ± standard deviation. The independent t-test was appointed to analyze data in (F-G). One-way ANOVA was appointed to analyze data in (H-I). Two-way ANOVA was appointed to analyze data in (D). Tukey's multiple comparisons test was employed for the post hoc test. \* $p < 0.05$ .

experiments with oe-LINC00261. It was observed that, under 4Gy X-ray radiation, TE-1-R cells in the si-DIRAS1 group exhibited decreased  $\gamma$ -H2AX levels ( $p < 0.05$ ; Figure 6B), elevated colony formation ( $p < 0.05$ ; Figure 6C), and reduced apoptosis ( $p < 0.05$ ; Figure 6D). Overall, these findings suggested that DIRAS1 depletion partially annulled the promotive effect of LINC00261 on EC cell radiosensitivity.

### LINC00261 Over-Expression Enhances EC Radiosensitivity in vivo

Lastly, we explored the effects of LINC00261 on EC radiosensitivity with the help of in vivo models. TE-1-R cells with stable oe-LINC00261 were injected into mice and subjected to 4 Gy X-ray radiation, after which mice with LINC00261 over-expression presented with declined tumor volume and weights ( $p <$



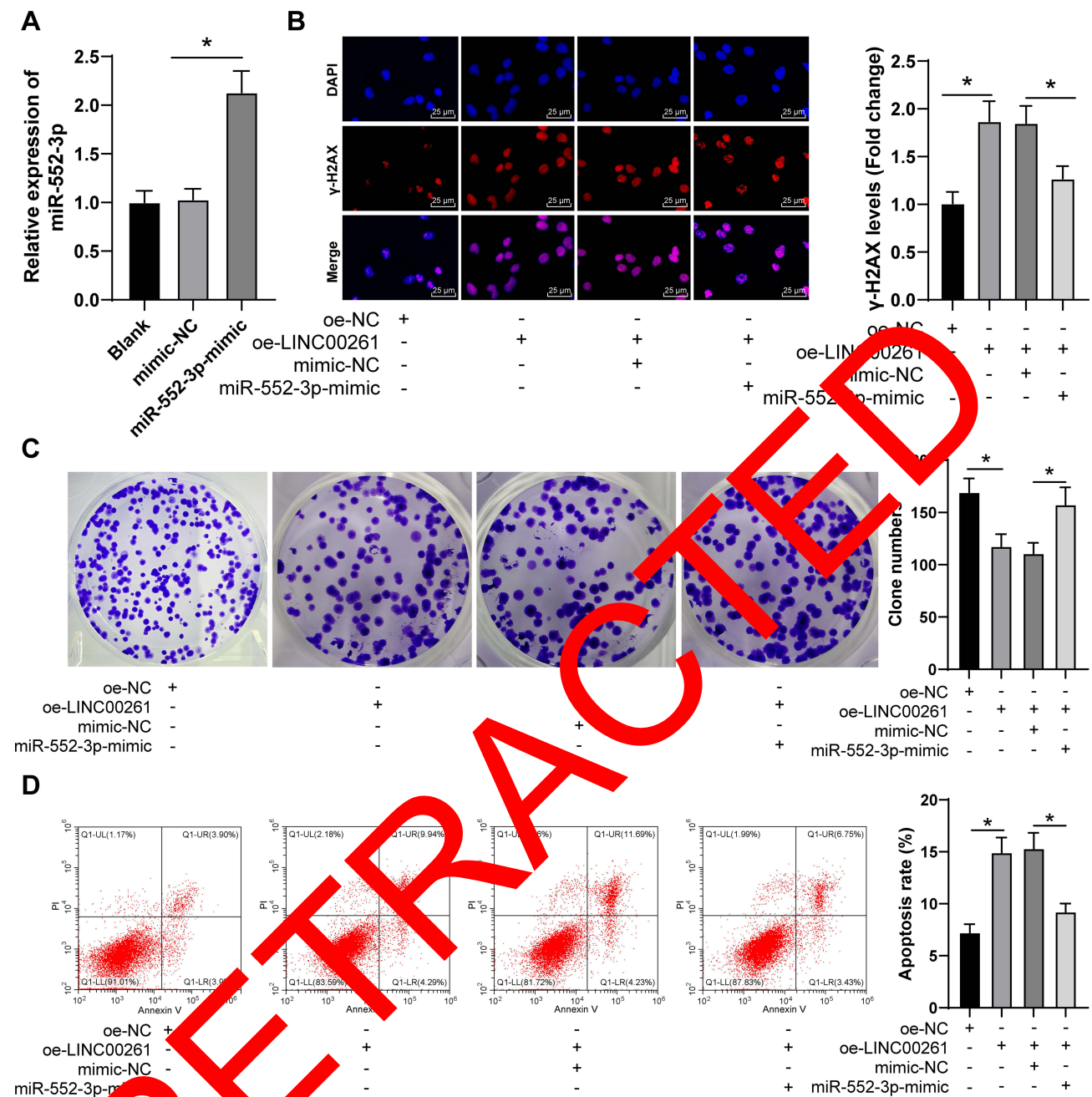


**Figure 4** miR-552-3p overexpression neutralizes the promotive effect of LINC00261 on EC cell radiosensitivity. miR-552-3p-mimic was transfected into TE-I-R cells, with mimic-NC as control. (A) miR-552-3p expression efficiency was examined by RT-qPCR, and the collaborative experiment of miR-552-3p-mimic and oe-LINC00261 was conducted under 4 Gy X-ray irradiation. (B)  $\gamma$ -H2AX levels in cells were determined by immunofluorescent staining. (C) Colony formation of cells was measured by colony formation assay. (D) Apoptosis of cells was determined by flow cytometry. The independent experiment was repeated 3 times. The measurement data were presented as mean  $\pm$  standard deviation. One-way ANOVA was appointed to analyze data in (A–D). Tukey’s multiple comparisons test was employed for the post hoc test. \* $p < 0.05$ .

0.05; Figure 7A and B), reduced miR-552-3p expression levels ( $p < 0.05$ ; Figure 7C), elevated DIRAS1 mRNA expression levels ( $p < 0.05$ ; Figure 7D), upregulated  $\gamma$ -H2AX levels, and down-regulated Ki67 expression levels ( $p < 0.05$ ; Figure 7E). Altogether, these findings indicated that LINC00261 enhanced EC radiosensitivity by

competitively binding to miR-552-3p to up-regulate DIRAS1 transcription.

### Discussion

As a life-threatening malignancy, EC is associated with ever-increasing morbidity and unsatisfying overall survival rates despite the advent of improved therapeutic

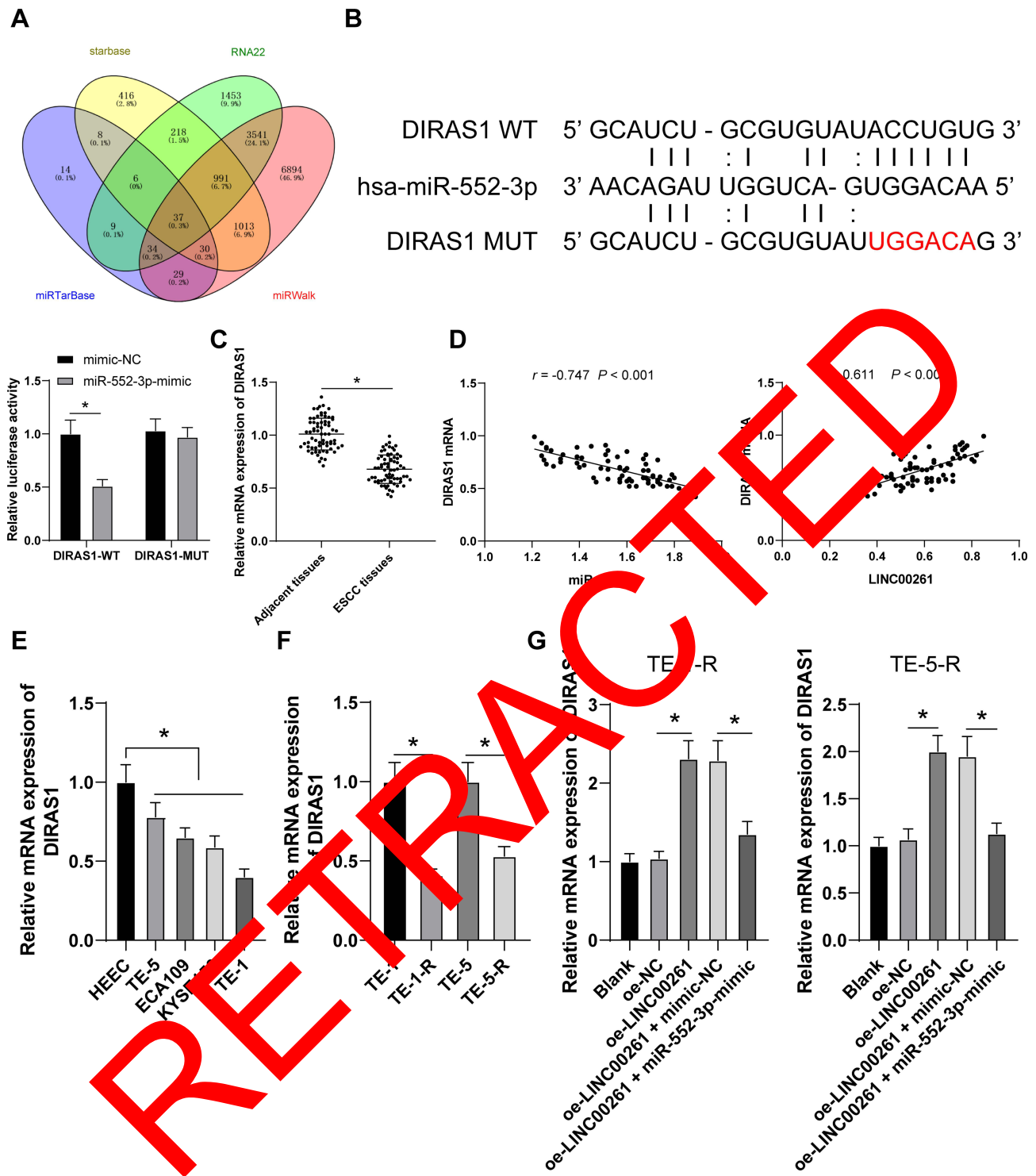


**Figure 5** miR-552-3p targets DIRAS1. (A) Target genes downstream of miR-552-3p were analyzed by Starbase, RNA22, miRTarBase, and miRWalk websites. (B) The binding relation between miR-552-3p and DIRAS1 was predicted by dual-luciferase reporter gene assay. (C) DIRAS1 expression in EC tissues was detected by RT-qPCR. (D) The correlation analysis of miR-552-3p and DIRAS1. (E and G) DIRAS1 expression in EC cells was verified via RT-qPCR. The independent experiment was repeated 3 times. The measurement data were presented as mean ± standard deviation. The t-test was appointed to analyze data in (C). One-way ANOVA was appointed to analyze data in (F and G). Two-way ANOVA was appointed to analyze data in (B). Tukey's multiple comparisons test was employed for the post hoc test. \* $p < 0.05$ .

interventions.<sup>4</sup> Radiotherapy is regarded as the most effective modality to treat EC, however, radioresistance therefrom can sabotage EC treatment and further escalate EC

malignancy.<sup>21</sup> Meanwhile, the hard-done work of our peers has indicated the use of LINC00261 as a tumor inhibitor in various cancers including EC, due to its ability

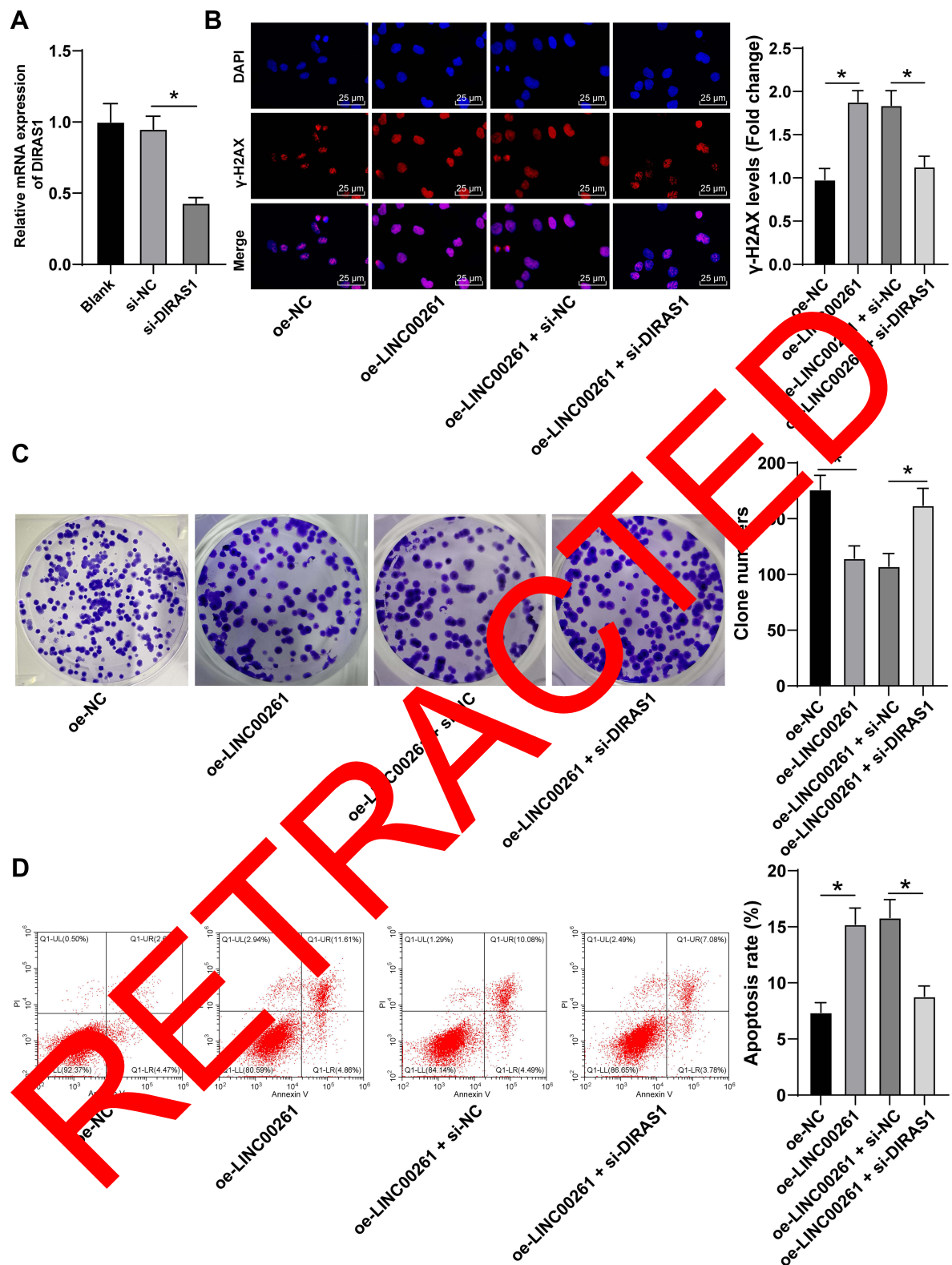


**Figure 6** DIRAS1 depletion partially annuls the promotive role of LINC00261 overexpression in EC cell radiosensitivity. si-DIRAS1 was transfected into TE-I-R cells, with si-NC as control. **(A)** Transfection efficiency was examined by RT-qPCR, and the collaborative experiment of si-DIRAS1 and oe-LINC00261 was conducted under 4 Gy X-ray radiation. **(B)**  $\gamma$ -H2AX levels in cells were determined by immunofluorescent staining. **(C)** Colony formation of cells was measured by colony formation assay. **(D)** Apoptosis of cells was determined by flow cytometry. The independent experiment was repeated 3 times. The measurement data were presented as mean  $\pm$  standard deviation. One-way ANOVA was appointed to analyze data in **(A–D)**. Tukey's multiple comparisons test was employed for the post hoc test. \* $p < 0.05$ .

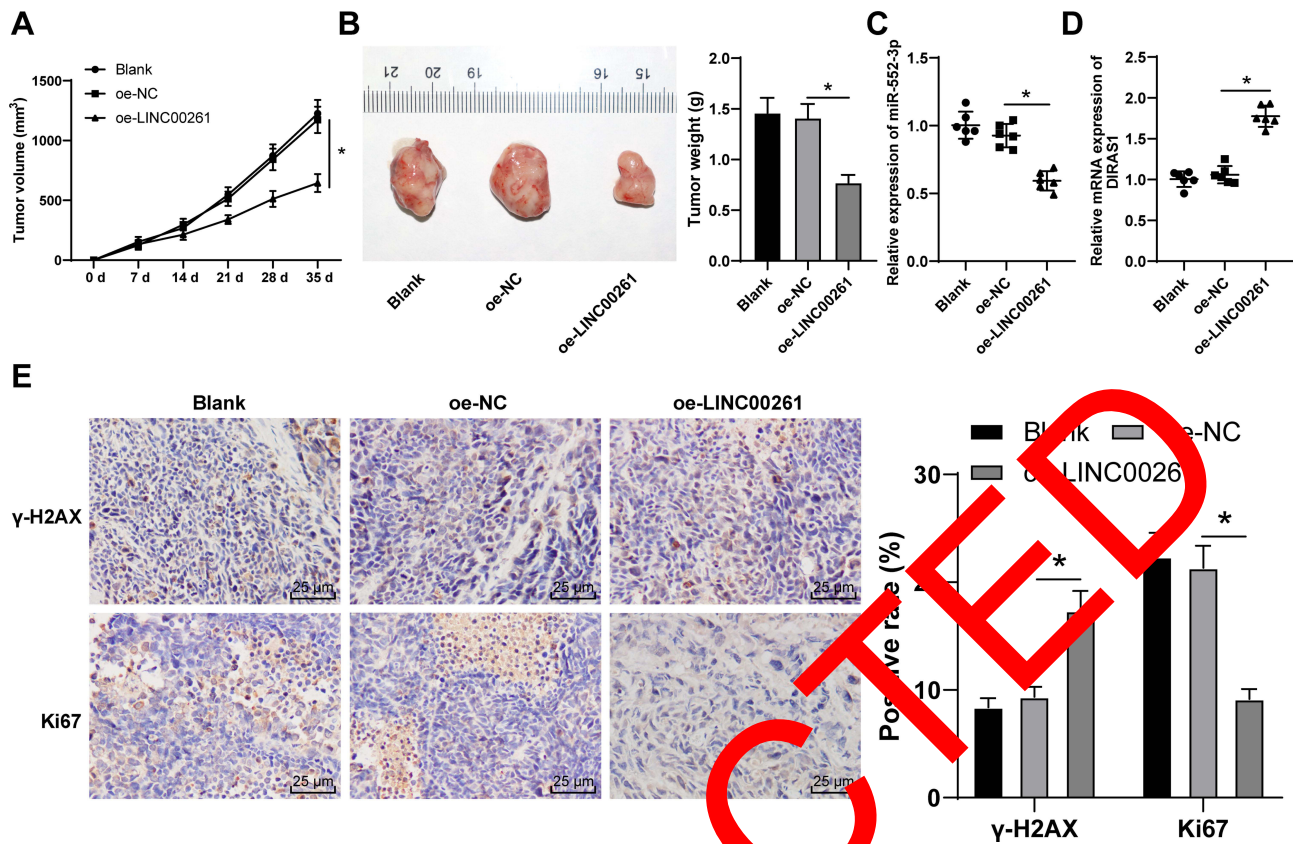


**Figure 7** LINC00261 overexpression enhances EC radiosensitivity in vivo. TE-1 cells with stable oe-LINC00261 were injected into mice. Tumor volume (A) and weight (B) were measured. (C and D) miR-552-3p (C), and DIRAS1 mRNA (D) expressions in mice tumor tissues were detected by RT-qPCR. (E)  $\gamma$ -H2AX and Ki67 expressions in tumors were measured by IHC. (A and B) N = 12; (C and D) N = 6. The measurement data were presented as mean  $\pm$  standard deviation. One-way ANOVA was appointed to analyze data in (B–D). Two-way ANOVA was appointed to analyze data in (A and E). Tukey’s multiple comparisons test was employed for the post hoc test. \**p* < 0.05.

to modulate cellular survival, death, development and proliferation in colon carcinoma and drug-resistant cells, chemoresistance as well as promoting prognostic consequences.<sup>22</sup> At this conjunction, we speculated if LINC00261 could serve as a benign indicator of EC, and subsequently explored the underlying interplay of LINC00261 in EC chemoresistance, aiming to provide novel insights for EC alleviation.

A wide range of lncRNAs are known to participate in EC progression by virtue of mediating the tumor-associated and therapeutic efficiency, and cell radioresistance and chemoresistance.<sup>23</sup> In our study, we found that LINC00261 was weakly-expressed in EC tissues and cells, while detection of LINC00261 expression patterns in radioresistant and parental EC cells illustrated that LINC00261 expression levels were further reduced in radioresistant cells. On the other hand, when LINC00261 was up-regulated in radioresistant cells via oe-LINC00261 treatment, we observed reductions in SF and colony formation, while  $\gamma$ -H2AX levels and apoptosis were augmented. Similarly, a prior study came across LINC00261

while over-expressing LINC00261 brought about quenched cell biological behaviors, encouraged apoptosis, and enhanced drug-sensibility.<sup>24</sup> In addition, down-regulation of LINC00261 has been previously documented in pancreatic adenocarcinoma, wherein these poor LINC00261 expressions were indicated to catalyze EC cell aggressiveness and migration.<sup>25</sup> Moreover, effective treatment of EC is characterized by partial-repression of EC malignancy and improvements in radiosensitivity, as well as elevated  $\gamma$ -H2AX levels, which suggests that  $\gamma$ -H2AX might predict alleviation of EC and is further associated with improved radiosensitivity of EC.<sup>26</sup> Meanwhile, apoptosis is a well-known process associated with cell death and self-renewal, whereas apoptosis deficiency can bring about exacerbated cancer development as it augments tumor growth and cell resistance to therapies.<sup>27</sup> Interestingly, a prior study uncovered that over-expression of LINC00261 inhibited EC growth, and further enhanced apoptosis and sensitivity to



5-fluorouracil, which is in accordance with our findings.<sup>10</sup> Furthermore, we carried out a series of *in vivo* experiments, which included inoculation of mice with TE-1-R cells with stable oe-LINC00261. Following treatment with 4 Gy X-ray radiation, we observed that mice with over-expressed LINC00261 presented with declined tumor volume and weights, up-regulated  $\gamma$ -H2AX levels, and down-regulated Ki67 expression levels. Altogether, these findings and evidence indicated that LINC00261 enhanced radiosensitivity in EC cells.

Furthermore, many miRs are implicated in the cell radioresistance of different carcinomas owing to their participation in the ceRNA network.<sup>28</sup> To further clarify the downstream mechanism of LINC00261, we predicted and analyzed the subcellular localization of LINC00261, which unveiled that LINC00261 was primarily localized in the cytoplasm, indicating that LINC00261 might modulate EC cell activities via the ceRNA network. Additionally, we explored the downstream targets of LINC00261, and came across miR-552-3p. It is also noteworthy that a prior study highlighted that LINC00261 could sabotage pancreatic cancer malignancy by targeting miR-552-3p.<sup>11</sup> In addition, another investigation illustrated that miR-552-5p served as a dangerous indicator for esophageal squamous cell carcinoma (ESCC) prognosis,<sup>29</sup> which reiterates the significance of miR-552-5p in EC. Moreover, our findings further illustrated that miR-552-3p was highly-expressed in EC cells, while also down-regulated in TE-1-R and TE-5-R cells relative to parental cells. Furthermore, miR-552-3p could be a target gene of

LINC00261. Besides, following transfection of miR-552-3p-mimic into EC radioresistant cells with oe-LINC00261 treatment, we observed that a decline in  $\gamma$ -H2AX levels, while cell colony was facilitated and apoptosis was quenched. In accordance with our findings, over-expressing miR-552 was previously revealed to enhance colony formation and cancer cell dissemination, while limiting radiosensitivity in colorectal cancer.<sup>30</sup> What's more, miR-552 exhaustion discouraged cell mobility, but improved apoptosis in hepatocellular carcinoma.<sup>31</sup> In general, the aforementioned findings indicated that miR-552-3p over-expression neutralized the promotive effect of LINC00261 on EC cell radiosensitivity.

Thereafter, we explored the downstream mechanism of miR-552-3p and focused our efforts on DIRAS1, which is a well-acknowledged cancer inhibitor as its over-expression consolidated the effect of anti-tumor drugs.<sup>32</sup> Even more so, DIRAS1 has been previously suggested to be capable of inhibiting ESCC progression.<sup>33</sup> Herein, our findings illustrated that DIRAS1 was poorly-expressed in EC cells, while also being down-regulated in TE-1-R and TE-5-R cells relative to parental cells. Besides, DIRAS1 could be a target gene of miR-552-3p. To further elucidate the effect of DIRAS1 on EC radiosensitivity, we transfected si-DIRAS1 into EC radioresistant cells with oe-LINC00261 treatment, and subsequent findings unveiled that silencing of DIRAS1 brought about diminished  $\gamma$ -H2AX levels, augmented colony formation, and restricted apoptosis. Moreover, another prior study manifested that DIRAS1 contributed to repressed colony formation and

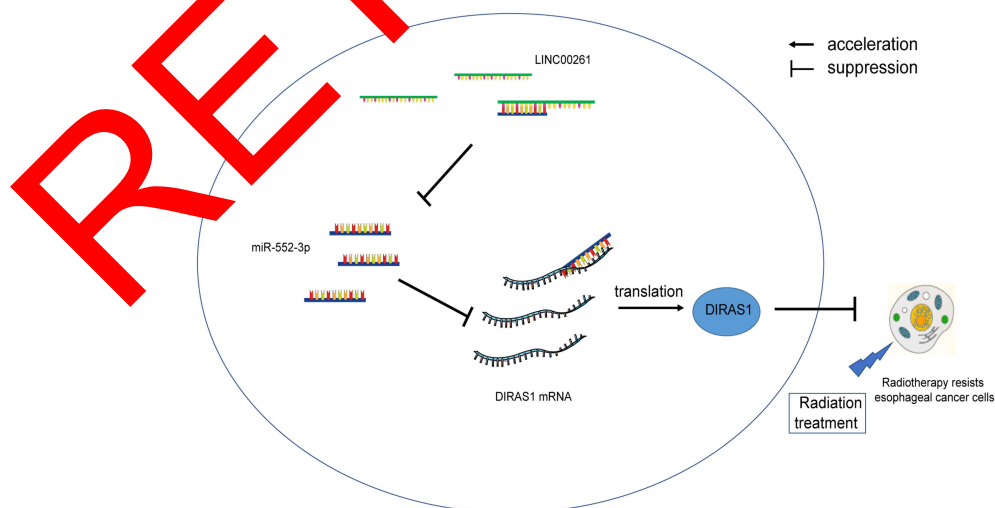


**Figure 8** The mechanism of the LINC00261/miR-552-3p/DIRAS1 ceRNA network in EC radioresistance. LINC00261 functioned as a ceRNA to competitively bind to miR-552-3p and upregulate DIRAS1 expression to repress EC radioresistance.

cell activities in ESCC.<sup>20</sup> In addition, DIRAS1 silencing is known to facilitate tumor growth, enhance cancer cell survival and metastasis, and further suppress apoptosis.<sup>34</sup> Overall, these findings and evidence indicated that DIRAS1 depletion partially annulled the promotive effect of LINC00261 on EC cell radiosensitivity.

## Conclusion

In word, the current study highlighted that LINC00261 functioned as a ceRNA to competitively bind to miR-552-3p and up-regulate DIRAS1 expression, resulting in repression of EC radioresistance (Figure 8). Our findings further suggested a therapeutic implication for EC alleviation. However, our study solely focused on the role of the LINC00261/miR-552-3p/DIRAS1 ceRNA network in EC radioresistance. We shall explore the possible upstream mechanism of LINC00261 and other downstream mechanisms in our future endeavors. Moreover, the experimental revelation and realistic application of our findings in clinical practice require extensive validation. Nevertheless, we hope the new-found significance of the LINC00261/miR-552-3p/DIRAS1 ceRNA network can contribute to EC research.

## Abbreviations

EC, esophageal cancer; LINC, long intergenic non-coding RNAs; miR, microRNA; SF, survival fraction; lncRNAs, long non-coding RNA; ceRNA, competing endogenous RNA; DIRAS1, DIRAS family GTPase-1LV, lentivirus; oe, overexpression; NC, negative control; si, small interfering; RT-qPCR, reverse transcription quantitative polymerase chain reaction; CCK-8, cell counting kit-8; FITC, fluorescein isothiocyanate; WT, wild type; MUT, mutant type; RIP, RNA binding protein immunoprecipitation; IHC, immunohistochemistry; ANOVA, analysis of variance; ESCC, esophageal squamous cell carcinoma.

## Data Sharing Statement

All the data generated or analyzed during this study are included in this published article.

## Ethics Approval and Informed Consent

This study was approved and supervised by the ethics committee of The Second Affiliated Hospital of Xi'an Jiaotong University. Informed consent was received from all subjects. The protocol was also approved by the

Institutional Animal Care and Use Committee of The Second Affiliated Hospital of Xi'an Jiaotong University and the Guidelines for the Care and Use of Laboratory Animals provisions of administration and usage of laboratory animals. Significant efforts were made to minimize both the number of animals and their respective suffering.

## Acknowledgments

We thank all members in our team for the excellent work.

## Disclosure

The authors report no conflicts of interest in this work.

## References

- Domper Arnal MJ, Hernandez Arenas A, Lanas Arbeloa A. Esophageal cancer: risk factors, screening and endoscopic treatment in Western and Eastern countries. *World J Gastroenterol.* 2015;21(26):7933–7941. doi:10.3748/wjg.v21.i26.7933
- Uhlenhuth EJ, Theisen LO, Sunkara Y, et al. Epidemiology of esophageal cancer: update in global trends, etiology and risk factors. *Clin J Gastroenterol.* 2020;13(10):1010–1021. doi:10.1007/s12328-020-00237-x
- Chhda M, Kuwano H. Current status and future prospects for esophageal cancer treatment. *Ann Thorac Cardiovasc Surg.* 2019;23(1):1–11. doi:10.5761/atcs.ra.16-00162
- Huang J, Yu SJ. Esophageal cancer: risk factors, genetic association, and treatment. *Asian J Surg.* 2018;41(3):210–215. doi:10.1016/j.asjsur.2016.10.005
- Sun DE, Ye SY. Emerging roles of long noncoding RNA regulator of reprogramming in cancer treatment. *Cancer Manag Res.* 2020;12:6103–6112. doi:10.2147/CMAR.S253042
- Su M, Xiao Y, Ma J, et al. Long non-coding RNAs in esophageal cancer: molecular mechanisms, functions, and potential applications. *J Hematol Oncol.* 2018;11(1):118. doi:10.1186/s13045-018-0663-8
- Eke I, Bylicky MA, Sandfort V, et al. The lncRNAs LINC00261 and LINC00665 are upregulated in long-term prostate cancer adaptation after radiotherapy. *Mol Ther Nucleic Acids.* 2021;24:175–187. doi:10.1016/j.omtn.2021.02.024
- Liu S, Zheng Y, Zhang Y, et al. Methylation-mediated LINC00261 suppresses pancreatic cancer progression by epigenetically inhibiting c-Myc transcription. *Theranostics.* 2020;10(23):10634–10651. doi:10.7150/thno.44278
- Zhou Z, Ma J. Expression and clinical significance of long-chain noncoding RNA LINC00261 in colon cancer. *Clin Lab.* 2019;65(12/2019):12. doi:10.7754/Clin.Lab.2019.190402
- Lin K, Jiang H, Zhuang SS, et al. Long noncoding RNA LINC00261 induces chemosensitization to 5-fluorouracil by mediating methylation-dependent repression of DPYD in human esophageal cancer. *FASEB J.* 2019;33(2):1972–1988. doi:10.1096/fj.201800759R
- Chen T, Lei S, Zeng Z, et al. Linc00261 inhibits metastasis and the WNT signaling pathway of pancreatic cancer by regulating a miR5525p/FOXO3 axis. *Oncol Rep.* 2020;43(3):930–942. doi:10.3892/or.2020.7480
- Yan D, Liu W, Liu Y, et al. LINC00261 suppresses human colon cancer progression via sponging miR-324-3p and inactivating the Wnt/beta-catenin pathway. *J Cell Physiol.* 2019;234(12):22648–22656. doi:10.1002/jcp.28831
- Qi X, Zhang D-H, Wu N, et al. ceRNA in cancer: possible functions and clinical implications. *J Med Genet.* 2015;52(10):710–718. doi:10.1136/jmedgenet-2015-103334

14. Zou Y, Zhao X, Li Y, et al. miR-552: an important post-transcriptional regulator that affects human cancer. *J Cancer*. 2020;11(21):6226–6233. doi:10.7150/jca.46613
15. Lai CH, Liang XZ, Liang XY, et al. Study on miRNAs in pan-cancer of the digestive tract based on the illumina HiSeq system data sequencing. *Biomed Res Int*. 2019;2019:8016120. doi:10.1155/2019/8016120
16. Li X, Liu S, Fang X, et al. The mechanisms of DIRAS1 family members in role of tumor suppressor. *J Cell Physiol*. 2019;234(5):5564–5577. doi:10.1002/jcp.27376
17. Zheng R, Gao D, He T, et al. Methylation of DIRAS1 promotes colorectal cancer progression and may serve as a marker for poor prognosis. *Clin Epigenetics*. 2017;9:50. doi:10.1186/s13148-017-0348-0
18. Jones-Bolin S. Guidelines for the care and use of laboratory animals in biomedical research. *Curr Protoc Pharmacol*. 2012;Appendix 4: Appendix 4B. doi:10.1002/0471141755.pha04bs59
19. Yanagawa M, Tatsumi M, Miyata H, et al. Evaluation of response to neoadjuvant chemotherapy for esophageal cancer: PET response criteria in solid tumors versus response evaluation criteria in solid tumors. *J Nucl Med*. 2012;53(6):872–880. doi:10.2967/jnumed.111.098699
20. Zhu YH, Fu L, Chen L, et al. Downregulation of the novel tumor suppressor DIRAS1 predicts poor prognosis in esophageal squamous cell carcinoma. *Cancer Res*. 2013;73(7):2298–2309. doi:10.1158/0008-5472.CAN-12-2663
21. Fei Z, Gu W, Xie R, et al. Artesunate enhances radiosensitivity of esophageal cancer cells by inhibiting the repair of DNA damage. *J Pharmacol Sci*. 2018;138(2):131–137. doi:10.1016/j.jphs.2018.09.011
22. Zhang M, Gao F, Yu X, et al. LINC00261: a burgeoning long noncoding RNA related to cancer. *Cancer Cell Int*. 2021;21(1):274. doi:10.1186/s12935-021-01988-8
23. Ghafouri-Fard S, Shoorei H, Dashti S, et al. Expression profile of lncRNAs and miRNAs in esophageal cancer: implications in diagnosis, prognosis, and therapeutic response. *J Cell Physiol*. 2020;235(12):9269–9290. doi:10.1002/jcp.29825
24. Wang ZK, Yang L, Wu LL, et al. Long non-coding RNA LINC00261 sensitizes human colon cancer cells to cisplatin therapy. *Braz J Med Biol Res*. 2017;51(2):e6793. doi:10.1590/1414-431X20176793
25. Dorn A, Glass M, Neu CT, et al. LINC00261 is differentially expressed in pancreatic cancer subtypes and regulates pro-epithelial cell identity. *Cancers*. 2020;12(5):1227. doi:10.3390/cancers12051227
26. Wu X, Smavadati S, Nordfjall K, et al. Telomerase antagonist imetelstat inhibits esophageal cancer cell growth and increases radiation-induced DNA breaks. *Biochim Biophys Acta*. 2012;1823(12):2130–2135. doi:10.1016/j.bbamer.2012.08.003
27. Wong RS. Apoptosis in cancer: from pathogenesis to treatment. *J Exp Clin Cancer Res*. 2011;30(1):87. doi:10.1186/1756-9966-30-87
28. Wu K, Hu Y, Yan K, et al. microRNA-10b confers cisplatin resistance by activating AKT/mTOR/P70S6K signaling via targeting PPARgamma in esophageal cancer. *J Cell Physiol*. 2020;235(2):1247–1258. doi:10.1002/jcp.29040
29. Shi X, Li Y, Sun Y, et al. Genome-wide analysis of lncRNAs, miRNAs, and mRNAs forming a prognostic scoring system in esophageal squamous cell carcinoma. *PeerJ*. 2020;8:e8368. doi:10.7717/peerj.8368
30. Kwak B, Kim DU, Kim TO, et al. MiR-552 links Wnt signaling to p53 tumor suppressor in colorectal cancer. *Int J Oncol*. 2018;53(4):1800–1808. doi:10.3892/ijo.2018.4503
31. Ma Y, Ma M, Ma L, et al. Downregulation of miR-552 in hepatocellular carcinoma inhibits cell migration and invasion, and promotes cell apoptosis via RhoA3. *Exp Ther Med*. 2019;18(5):3829–3836. doi:10.3892/etm.2019.8061
32. Verma SP, Agarwal A, Das S. Sodium butyrate induces cell death by autophagy and reactivation of tumor suppressor gene DIRAS1 in renal cell carcinoma cell line CCK14. *In Vitro Cell Dev Biol Anim*. 2018;54(4):299–303. doi:10.1007/s11626-018-0239-5
33. Bergom C, Plesser AD, Rymaszewski A, et al. The tumor suppressive small GTPase DiRas1 binds the noncanonical guanine nucleotide exchange factor SmgGDS and antagonizes SmgGDS interactions with oncogenic small GTPases. *J Biol Chem*. 2016;291(12):6534–6545. doi:10.1074/jbc.M115.696831
34. Xu X, Li J, Zhang S, et al. RNAi and vector-mediated overexpression of DIRAS1 suppresses tumor growth and migration in renal cell carcinoma. *Mol Ther Nucleic Acids*. 2018;12:845–853. doi:10.1016/j.mtn.2018.07.019